

Legacy base metal slags can generate toxic leachates

Adijat T. Awoniran,^{1,a)} Annelly Ketheson,² Sandra Piazzolo,^{2,3} and Damian B. Gore¹

¹Department of Environmental Sciences, Macquarie University, Sydney 2109, Australia

²Department of Earth and Planetary Sciences, Macquarie University, Sydney 2109, Australia

³School of Earth and Environment, University of Leeds, Leeds LS2 9JT, UK

(Received 7 April 2017; accepted 15 August 2017)

Slags sourced from a derelict zinc–lead–copper–silver–tungsten mine were examined for their bulk elemental composition and mineralogy. pH, oxidation–reduction potential, and the leachability of selected elements (sulphur, calcium, iron, copper, zinc, and lead) were assessed during a 130-day deionised water extraction conducted under oxic conditions. Slags were rich in silicon, iron, copper, zinc, and lead, hosted within minerals including quartz (SiO₂), goethite [FeO(OH)], augite [Ca(Mg, Al, Fe)Si₂O₆], and lead (Pb⁰). Leachates from the slags increased in analyte concentration throughout the 130-day experiment, with iron, copper, zinc, and lead attaining >5 mg l⁻¹ in some samples. These findings indicate that this pyrometallurgical waste should not be considered environmentally inert, as leachates emanating from them in the field might pose a significant risk to the environment. © 2018 International Centre for Diffraction Data. [doi:10.1017/S0885715617000999]

Key words: slag, derelict mines, leachability, mineralogy, elemental composition

I. INTRODUCTION

Slag is a waste product of pyrometallurgical processing to recover metals. At many older mines, slag was intentionally dumped near the furnaces that created it, leaving behind coherent piles or jumbles of slag weighing many thousands of tonnes. Its appearance depends on its chemistry and rate of cooling using air or water, which affects the crystallinity, creating variation in mineralogy, texture, colour, porosity, inclusions, and specific gravity (Bachmann, 1982; Panayotova *et al.*, 2015; Piatak *et al.*, 2015). Slags can be vesicular because of the activity of fluids such as steam during cooling and solidification after smelting. These voids help to make slag porous and in places, permeable, allowing environmental water to infiltrate and leachate to exfiltrate. Slag from base metal ores is composed of minerals including silicates such as olivine [fayalite (FeSiO₄), tephroite (MnSiO₄)], pyroxene [diopside (CaMgSi₂O₄)], augite [Ca(Mg, Al, Fe)Si₂O₆], quartz (SiO₂), and white mica [muscovite KAl₂(SiAl)₄O₁₀(H₂O)]; oxides [spinel (MgAl₂O₄), hematite (Fe₂O₃)]; and sulphides [galena (PbS), pyrite (FeS₂)], which vary from mine to mine (Lottermoser, 2002; Piatak *et al.*, 2004; Ströbele *et al.*, 2010). Slags are then subjected to chemical weathering, in some places creating secondary minerals which effloresce at the surface of small overhangs and/or under cobbles.

Many types of mine waste, particularly water, waste rock, and tailings, have been examined for their environmental impacts including acid mine drainage, mobility of toxic metals, formation of hardpans, and efflorescence of secondary minerals (Lottermoser, 2002; Johnson and Hallberg, 2005; Ströbele *et al.*, 2010; Morrison *et al.*, 2016). Yet, limited research has been reported on the environmental impacts of slags, possibly because metals are assumed to be encapsulated

and thus immobilised within a low-solubility glassy matrix. Possibly as a consequence, granulated slags have been used as filling for driveways, landscaping, drainage projects, gardens, and parks (Xue *et al.*, 2006; Morrison and Gulson, 2007; Mahieux *et al.*, 2009; Kelly, 2015). However, slags from derelict mines may contain high concentrations of Cu, Zn, As, and Pb-bearing minerals, and may also generate acidic, metal-bearing leachate when exposed to oxidation, followed by rainfall or soil water (Ettler *et al.*, 2009; Piatak *et al.*, 2015). Acidic leachates are formed by sulphide oxidation and are characterised by low pH and high conductivity, iron and sulphate. This acidic water can dissolve minerals and metals (Piatak *et al.*, 2004), which can then flow off, infiltrating soil and sediment, and contaminating surface water (creeks, rivers), groundwater, soil, and plants (Banks *et al.*, 1997; Romero *et al.*, 2006). The toxicity and bioaccessibility of these metals depend on the pH, redox potential, organic matter content, concentration, particle size, and nature of the environmental receptors (Julli, 1999; Strömberg and Banwart, 1999; Morrison and Gulson, 2007).

Soil, sediment, and mine waste have been characterised in many locations for their elemental composition, mineralogy, and leachability using different analytical methods (e.g. Gore *et al.*, 2007; Martínez-Sánchez *et al.*, 2008; Fryirs and Gore, 2013). Mineralogy and mineral morphology provide information on susceptibility to acid generation and liberation of metallic elements (Parbhakar-Fox *et al.*, 2013). Slags are composed of amorphous compounds and crystalline minerals. Standard methods of analysis are powder X-ray diffractometry (XRD) for mineralogy, and X-ray fluorescence (XRF) spectrometry, scanning electron microscopy with backscattered electron imaging and energy-dispersive spectrometry (SEM-EDS) for elemental composition and vibrational spectroscopy (e.g. Fourier-transform infrared spectroscopy) to determine bonds and help infer dominant phases (Ettler *et al.*, 2009; Ströbele *et al.*, 2010; Piatak *et al.*, 2015; Chand

^{a)}Author to whom correspondence should be addressed. Electronic mail: adijat.awoniran@students.mq.edu.au

et al., 2016; Morrison *et al.*, 2016). Constraining the leachability of metals from slag is important for understanding potential and actual impacts on the environment. This paper reports the bulk elemental composition, bulk mineralogy, distribution of minerals at the microscopic scale, and the leachability of selected elements from slags collected at a derelict zinc–lead–copper–silver–tungsten mine in order to help predict the potential threat of acid mine drainage and future liberation of metals to the environment. Of the sample characteristics measured, mineralogy and mineral solubility are fundamental to understanding the potential environmental threat.

II. MATERIALS AND METHODS

A. Study area and sampling

The derelict Cordillera mine, 50 km south of Bathurst and 42 km north of Crookwell, NSW, was a zinc–lead–copper–silver–tungsten deposit worked from 1887 to 1928 (DIGS, 1976). The geology consists of pyritic shales within acid volcanics. The primary minerals recorded include anglesite (PbSO_4), arsenopyrite (FeAsS), cuprotungstite [$\text{Cu}_2(\text{WO}_4)(\text{OH})_2$], galena (PbS), quartz (SiO_2), and sphalerite (ZnS) (DIGS, 1976; MINDAT, 2017). The ores were concentrated and smelted on site, leading to a diversity of solid phase mine waste. In the field, slags were present as discrete clasts in the shape of the former crucibles where they were air-cooled en route from the furnaces to the dumping area (Figure 1). Within this jumble, individual slag pieces ranged from glassy to vesicular or crystalline, and massive to fractured and porous. Five slags, representing massive, blocky, vesicular, and fractured textures were sampled and crushed to $<63 \mu\text{m}$ before milling.

B. Characterisation of slags

The elemental compositions of unprepared slags were measured using a handheld Olympus Delta Pro XRF spectrometer with 50 kV tantalum anode tube, with three measurement conditions of 20 s each in soil calibration mode. Inaccuracy, constrained via repeated measurement of NIST standard reference material SRM2710a, was generally around 1%, except for Fe which had $\sim 10\%$ analytical inaccuracy. Mineralogy was determined on samples of slag that were



Figure 1. (Colour online) Field occurrence of slag as blocky, porous jumbles at Cordillera mine, NSW (photo courtesy Peter Johnston).

powdered using a McCrone mill. The mill was cleaned using quartz sand followed by an ethanol wipe between each preparation. Samples were mounted on a silicon crystal low background holder, and diffractograms were collected from 5° to $90^\circ 2\theta$ using a PANalytical X'Pert Pro MPD diffractometer, using 45 kV, 40 mA, $\text{CuK}\alpha$ radiation scanning at $5^\circ 2\theta \text{ min}^{-1}$. Identification of the minerals was undertaken using PANalytical's HighScore Plus v2.2.4 software, with ICDD PDF2 and PAN-ICSD databases. Detection limits depend on crystallinity but are typically around 0.1–0.5 wt %. Slag fragments were embedded in epoxy, polished and carbon coated for the determination of mineral morphology and elemental composition using scanning electron microscopy. This was undertaken using a Hitachi TM3030 SEM with four-segment backscattered electron detector with Bruker Quantax 70 EDS detector and software. Energy-dispersive spectrometry was collected on carbon-coated samples using four Bruker X-flash detectors with 128 eV resolution, at 15 kV, 1850 mA filament current and 100 s live time.

C. Leachability of slags

A modified version of the Australian Synthetic Leaching Procedure (ASLP; Standards Australia, 1997) was used to examine the leachability of the slags. A weight of 10.0 g of slag sand ($\leq 2 \text{ mm}$ particle size) was placed in a 250 ml high-density polyethylene (HDPE) wide mouth bottle with 200 ml type 1 (ASTM, 1991) deionised water. Bottles were loosely fitted with a cap to allow oxic conditions throughout the experiment. Bottles were placed on a Ratek orbital shaker and at set times (0.02, 0.04, 0.13, 0.25, 1.0, 2.0, 3.5, 7.0, 14, 30, 60, and 130 days), solution pH and oxidation–reduction potential (ORP) were measured with a Denver Instrument model 250 m. At each sampling interval, 1.3 ml of leachate was withdrawn using a syringe, and filtered through a $0.45 \mu\text{m}$ pore size Sartorius MiniSart cellulose acetate syringe filter into a pre-acidified HDPE bottle. Fifty microlitres of 20 mg l^{-1} gallium spike was added to 450 μl of the sample and mixed on a vortex mixer for 15 s. Ten microlitres of the spiked acidified sample was placed on a pre-labelled siliconised quartz disc, and dried on a hot plate at 60°C for 15 min. Compositions of the evaporites on the discs were measured for elemental composition using a Bruker Picofox total reflection XRF spectrometer with molybdenum anode tube, and measurement conditions of 30 kV, no filter and a measurement time of 600 s. Limits of quantification are dependent on the matrix but were typically $\sim 5 \mu\text{g l}^{-1}$ for elements in this study. Inaccuracy, constrained using a Merck XVI multi-element standard, was better than 20% where concentrations exceeded 0.1 mg l^{-1} .

III. RESULTS

A. Slag descriptions: general

The slags were highly variable in appearance in the field; some were grey to black, while others were a reddish-brown colour. The reddish-brown colour reflected the presence of sulphides which are readily oxidised. At the outcrop scale, the slag varied from coherent masses, to individual cobble-size clasts formed by cooling of the slag before emplacement in the slag pile, with an estimated porosity exceeding 50%. In hand specimen, some slags were glassy, angular, and even obsidian-like

TABLE I. Slag elemental composition.

Analyte	Certified (mg kg ⁻¹)	Measured (mg kg ⁻¹)	Inaccuracy (%)	Slag A (wt%)	Slag B (wt%)	Slag C (wt%)	Slag D (wt%)	Slag E (wt%)
S	No value			0.12	0.18	0.16	0.45	0.23
Ca	9640	9547	1.0	0.053	0.036	0.058	0.086	6.86
Fe	43 200	47 479	9.9	12	14	36	38	10
Cu	3420	3434	0.4	0.28	0.35	0.026	0.058	0.26
Zn	4180	4226	1.1	1.26	1.13	0.15	0.094	0.97
Pb	5525	5485	0.7	1.40	2.51	0.015	0.028	1.96

The Standard Reference Material NIST 2710a was measured 22 times over the experimental period and yielded inaccuracies generally ~1% for the analytes measured here, except for Fe which had ~10% analytical inaccuracy.

on the surface with some internal open channels. The pores in these cases were disconnected from each other, so the permeability in these materials would be low. In other samples, vesicles of <1 to 5 mm diameter were evident both on the surface and in cross-section in the polished block mounts. In some cases, there were distinctive reaction rinds, which coupled with internal fractures would contribute to the effective porosity.

B. Elemental composition

The bulk elemental compositions of the slags (Table I) showed substantial heterogeneities having iron concentrations in slags A, B, C, D, and E between 10 and 38 wt%, and large variability in the concentration of other elements measured. Copper, zinc, and lead were abundant in slags A, B, and E but not in slags C and D (Table I). The spatial distributions of the elements (Figures 2 and 3) showed that many elements are finely dispersed in the matrix, although occasional larger grains rich in S and Pb (presumably galena) can be seen, for example, at the lower left of slag A (Figure 3).

C. Mineralogy

Slags were mainly composed of silicate and oxide minerals. Minerals identified from the slags by powder diffraction

were quartz (SiO₂), iron oxide hydrate (Fe₂O₃ · H₂O), augite [Ca(Mg,Al,Fe)Si₂O₆], and diopside [CaMg(Si₂O₆)] with lesser amounts of muscovite [KAl₂(SiAl)₄O₁₀(H₂O)], cristobalite (SiO₂), crednerite [Cu(Mn_{0.96}Cu_{0.04}O₂)], litharge (PbO), zircon (ZrO₂), and elemental lead (Pb⁰) (Table II, Figure 4). The silicate minerals predominantly contain Al, Mg, Mn, and Zn. Quartz was the most abundant mineral present in all five samples (A–E), and goethite, iron oxide hydrate, and augite were the iron-bearing minerals present in three samples (B–D). Background scatter on the diffractograms for slags B–E (Figure 4) indicate the presence of amorphous compounds; their amounts were not quantified.

C. Leachate chemistry

All slag leaching solutions started with deionised water with pH of 5.89. At the first sampling at 0.02 days (0.5 h), the solution had a lower pH of 3.6 and 4.3. After 6 h, leachates from slags A, B, and E increased in pH to between 6.44 and 6.73, while the pH of slags C and D leachates remained low for all sample measurements (Figure 5). Samples C and D displayed high values of ORP which increased through the experiment, while slags A, B, and E had lower ORP values (Figure 5).

By day 2, slag D had the greatest concentration of S (45.6 mg l⁻¹), which decreased to 17.8 mg l⁻¹ by the end

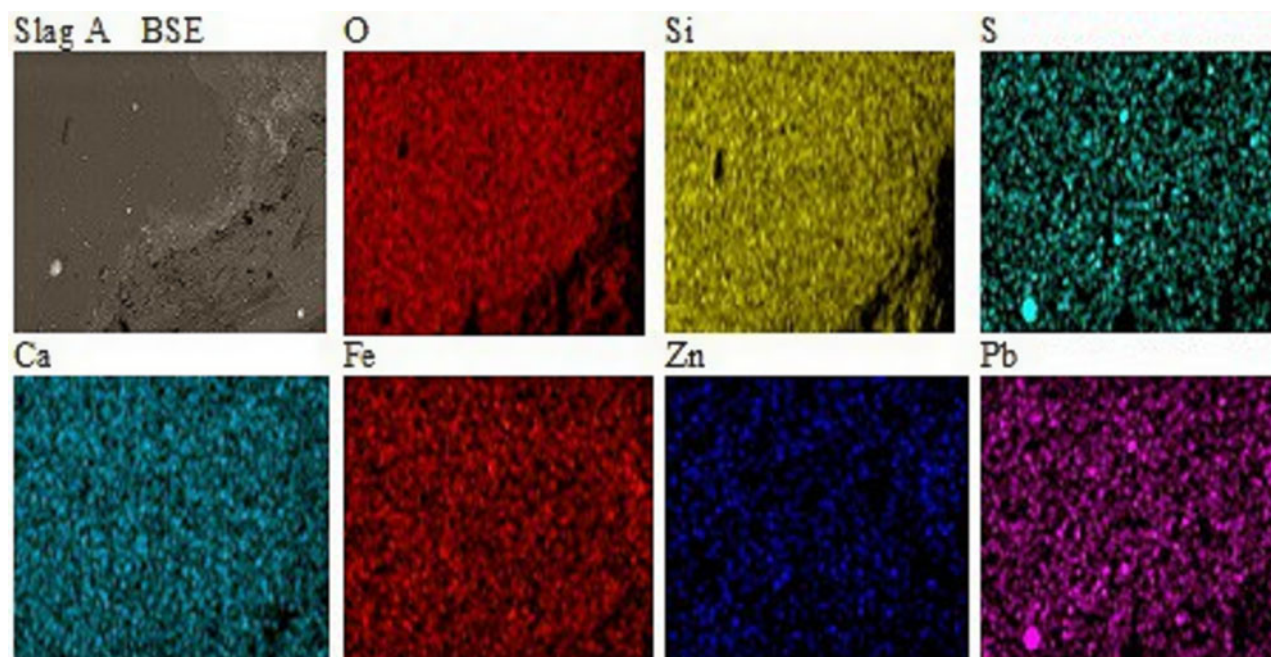


Figure 2. (Colour online) SEM micrographs with back-scattered electron and elemental maps of slag A. Images are 300 × 300 μm.

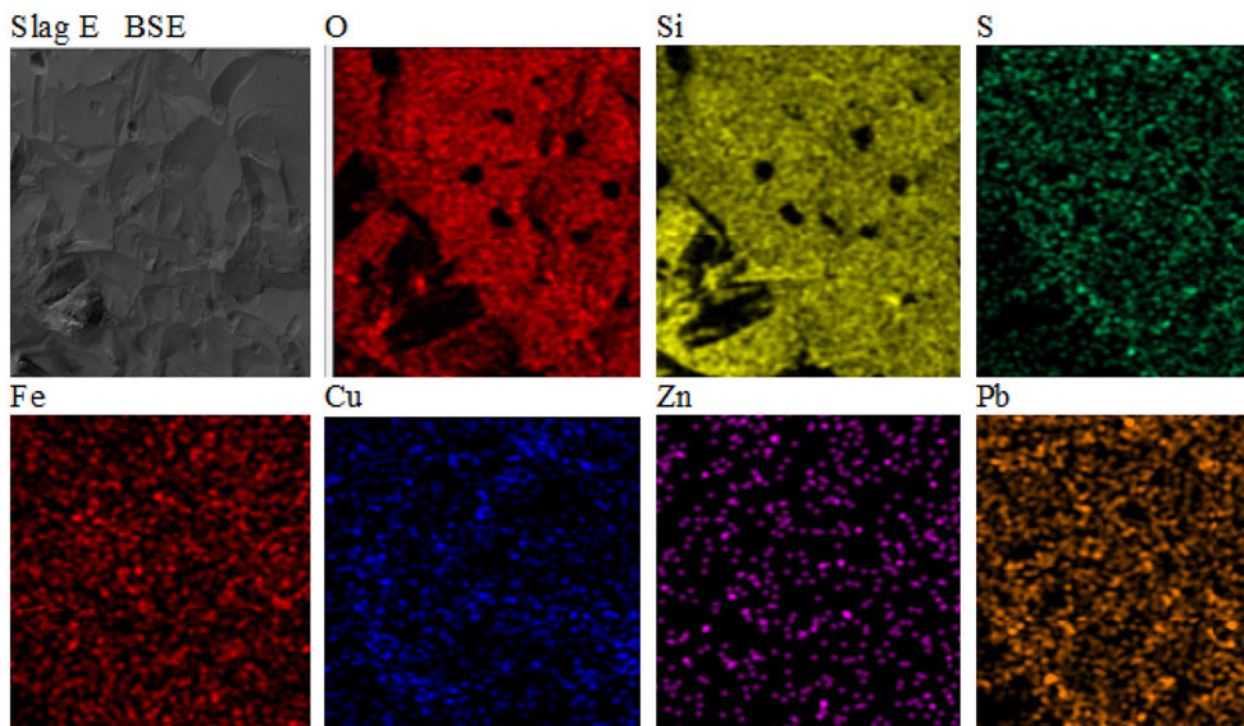


Figure 3. (Colour online) SEM micrographs with back-scattered electron and elemental maps of slag E. Images are $300 \times 300 \mu\text{m}^2$.

of the experiment. Slags A–C, and E had lower concentrations of S with little variation observed over 130 days [Figure 6(a)]. At the end of 130 days, slags A–C, and E had a concentration of Ca $>2.5 \text{ mg l}^{-1}$ [Figure 6(b)], while slag D released the lowest concentration (1.9 mg l^{-1}). Fe concentration was greatest in slag B [5 mg l^{-1} ; Figure 6(c)], while for slags A and C–E, the Fe concentration was low in comparison to their bulk mineralogy. Cu concentrations increased in all slags over time [Figure 6(d)] and were greatest for slag D at 5.3 mg l^{-1} . All slag solutions increased in Zn concentration over time, although slags C and D were exceptional with Zn concentrations $>3 \text{ mg l}^{-1}$ by the end of the 130-day experiment [Figure 6(e)]. Pb leachability was greatest in slag B [Figure 6(f)], while slags A and C–E showed much lower leachability for Pb, with concentrations $<1.6 \text{ mg l}^{-1}$. Comparison of the composition of the slags versus the

composition of the leachate after 130 days shows that the concentration of the metals Cu, Zn, and Pb in the solutions exhibits only a weak association with the bulk elemental composition (Figure 7).

IV. DISCUSSION

Elemental compositions measured using XRF spectrometry and SEM-EDS showed that many metals remained in the slags following processing. XRD showed that not all solid phases are amorphous, with a range of minerals including zero valent lead being present. Although all slags leached copper, zinc, and lead at different concentrations throughout the 130-day experiment, host minerals for all of these elements were not always able to be identified using XRD (Figure 4). Elemental maps show occasional grains of what might be

TABLE II. Qualitative slag mineralogy, using X-ray diffractometry.

Sample	Mineral family/reference code	Mineral	Chemical formula
Slag A	Silica/PDF 00-003-0427 (ICDD, 1953)	Quartz	SiO_2
	Metal/PDF 01-072-6646 (ICDD, 2003)	Lead	Pb^0
Slag B	Pyroxene/PDF 00-024-0202 (ICDD, 1974)	Augite	$\text{Ca}(\text{Mg,Al,Fe})\text{Si}_2\text{O}_6$
	Pyroxene/PDF 01-083-1817 (ICDD, 1981)	Diopside	$\text{CaMg}(\text{Si}_2\text{O}_6)$
	Oxide/PDF 98-005-9049 (ICSD, 2000)	Zircon	ZrO_2
	Metal/ICDD 00-004-0686 (ICDD, 1953)	Lead	Pb^0
Slag C	Silica/PDF 00-003-0419 (ICDD, 1953)	Quartz	SiO_2
	Oxide/PDF 98-002-1579 (ICSD, 1983)	Litharge	PbO
	Oxide/PDF 01-080-2974 (ICDD, 2011)	Crednerite	$\text{Cu}(\text{Mn}_{0.96}\text{Cu}_{0.04}\text{O}_2)$
	Hydroxide/PDF 00-002-0272 (ICDD, 1952)	Iron oxide hydrate	$\text{Fe}_2\text{O}_3 \cdot \text{H}_2\text{O}$
Slag D	Mica/PDF 00-058-2035 (ICDD, 2008)	Muscovite	$\text{KAl}_2(\text{SiAl})_4\text{O}_{10}(\text{H}_2\text{O})$
	Silica/PDF 01-070-3755 (ICDD, 2000)	Quartz	SiO_2
Slag E	Hydroxide/PDF 98-011-1234 (ICSD, 2008)	Goethite	$\text{FeO}(\text{OH})$
	Silica/PDF 01-071-0785 (ICDD, 1992)	Cristobalite	SiO_2
	Silica/PDF 98-001-2468 (ICSD, 1977)	Quartz	SiO_2

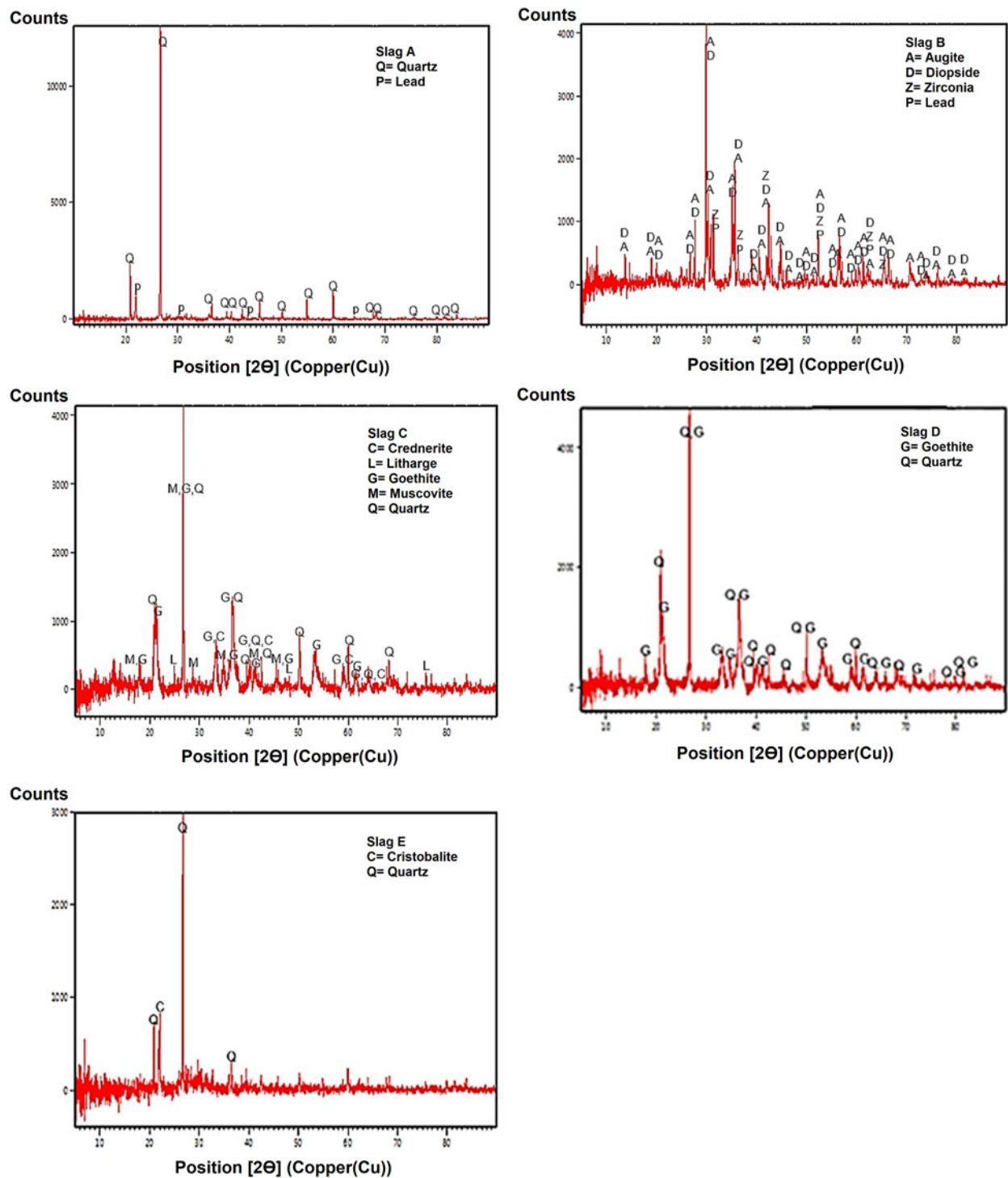


Figure 4. (Colour online) X-ray diffractograms for slags A–E. The dominant peaks for the different mineral phases found have been labelled.

galena, such as in the lower left of slag A (Figure 1). Galena and anglesite (PbSO_4) have been recorded from Cordillera mine; however, the absence of oxygen on the grain at lower left in Figure 1 indicates that the mineral there is not massicot or litharge (both PbO) or anglesite. Such remnant grains of galena suggest inefficient processing of the ore, helping to explain the large metal contents of some slags (Table I). The high oxygen contents in the elemental maps indicate that many elements exist in oxidised forms, consistent with the mineralogies identified.

The pH of leachates from slags A, B, and E climbed through the 130 days *in vitro* deionised water extraction from <5 to >6, whereas slags C and D remained with pH between 3.71 and 4.14. ORP reached a minimum at 1–3 days for A–E, probably reflecting early oxygen consumption, but this was followed by a rapid increase in the ORP of the samples. The large value of ORP affects the mobility, concentration, and fate of the metals in the leaching solution. The ranges in pH and ORP (Figure 5) throughout the experiment are consistent with the increases of metals in solution

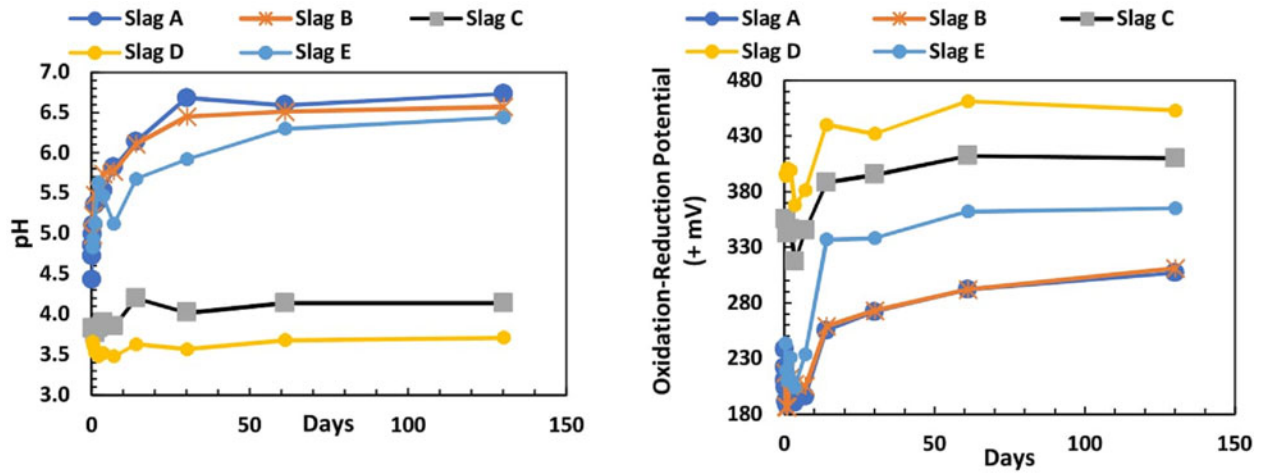


Figure 5. (Colour online) Leachate pH and ORP from all slags over 130 days.

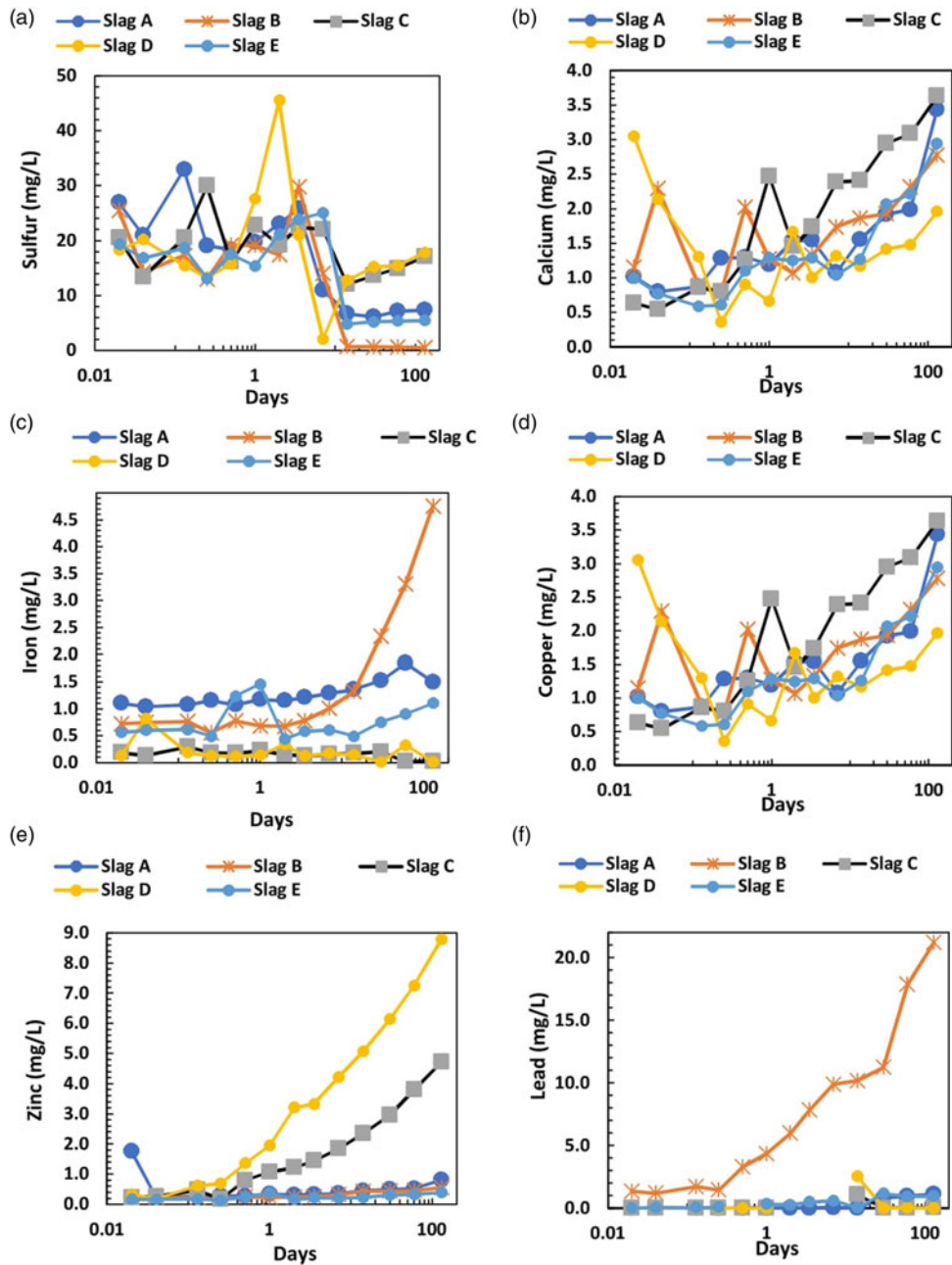


Figure 6. (Colour online) Concentrations of elements from leachates created over 130 days.

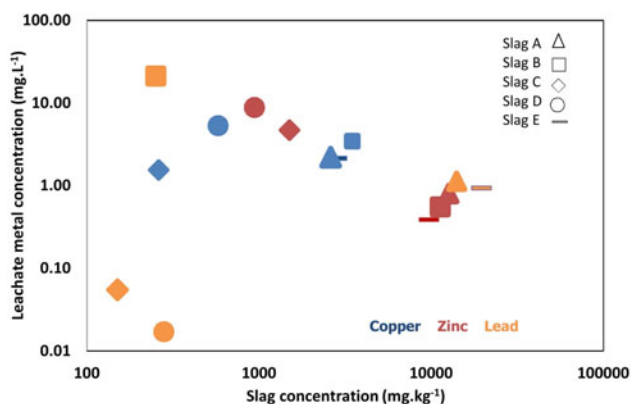


Figure 7. (Colour online) Concentrations of Cu, Zn, and Pb in the slag and the corresponding concentrations in the leachate at 130 days.

(Takeno, 2005). The low pH in slags C and D enhances the leachability of the metals, resulting in a good correlation between the metal concentrations in bulk-to-leached solutions from slags C and D.

Generally, the concentrations of elements in leachates from slags A to E are in the order of $S > Pb > Zn > Cu > Fe > Ca$, and most concentrations peaked near the end of the experiment (Figure 6). The concentrations of the metals Cu, Zn, and Pb in the solutions exhibit a weak association with the slag bulk elemental compositions (Figure 7). Reasons for this weak association might include variability in the permeability of the slag samples, or differences in the mineralogy or surface area of the minerals present, with resultant changes in fluid composition and pH.

Although the extraction efficiency is relatively low, the large concentration of metals in the slags means that the concentration of metals in the leachates might be significant for some organisms, particularly where those metals act in concert (e.g. Cooper *et al.*, 2009). Leachates from slags, therefore, deserve greater attention and scrutiny in order to determine their concentrations and ecotoxicological effects in the field.

V. CONCLUSIONS

Slags from a derelict base metal mine were characterised for their mineralogy and elemental composition. Leachates from the slags were characterised during a 130-day deionised water extraction. The authors have shown that slags can leach metals, and as a consequence have a potential environmental impact and should not be considered environmentally inert. Further research might reveal whether or not leachates from these and other slags exceed guidelines for the protection of aquatic ecosystems.

ACKNOWLEDGEMENTS

The authors thank Malvern PANalytical and Macquarie University for financial support under Grant No. 9201600948, and Russell Field and Armin Kavehei (Macquarie University) for laboratory assistance. Part of this research was conducted at the OptoFab node of the Australian National Fabrication Facility (ANFF), using National Collaborative Research

Infrastructure Strategy and New South Wales State Government funding.

- American Society for Testing and Materials (ASTM) D1193-91. (1991). Water quality standards. Accessed 06 April 2017 <http://www.muszeroldal.hu/assistance/waterstandards.pdf>.
- Bachmann, H.-G. (1982). *The Identification of Slags from Archaeological Sites* (Routledge, New York).
- Banks, D., Younger, P. L., Arnesen, R.-T., Iversen, E. R., and Banks, S. B. (1997). "Mine-water chemistry: the good, the bad and the ugly," *Environ. Geogra.* **32**, 157–174.
- Chand, S., Biswajit, P., and Kumar, M. (2016). "A comparative study of physicochemical and mineralogical properties of LD slag from some selected steel plants in India," *J. Environ. Sci. Technol.* **9**, 75–87.
- Cooper, N. L., Bidwell, J. R., and Kumar, A. (2009). "Toxicity of copper, lead, and zinc mixtures to *Ceriodaphnia dubia* and *Daphnia carinata*," *Ecotoxicol. Environ. Safety* **72**, 1523–1528.
- Digital Imaging Geological System (DIGS). (1976). Cordillera Mine, Tuena, Gunning. Accessed 30 Mar 2017. <https://search.geoscience.nsw.gov.au/report/R00045002?q=cordillera%20mine&sort=score%20desc&t=all&a=true&p=false&s=false>.
- Ettler, V., Johan, Z., Křibek, B., Šebek, O., and Mihaljevič, M. (2009). "Mineralogy and environmental stability of slags from the Tsumeb smelter, Namibia," *Appl. Geochem.* **24**, 1–15.
- Fryirs, K., and Gore, D. (2013). "Sediment tracing in the upper Hunter catchment using elemental and mineralogical compositions: implications for catchment-scale suspended sediment (dis)connectivity and management," *Geomorphology* **193**, 112–121.
- Gore, D. B., Preston, N. J., and Fryirs, K. A. (2007). "Post-rehabilitation environmental hazard of Cu, Zn, As and Pb at the derelict Conrad Mine, eastern Australia," *Environ. Pollut.* **148**, 491–500.
- Johnson, D. B., and Hallberg, K. B. (2005). "Acid mine drainage remediation options: a review," *Sci. Total Environ.* **338**, 3–14.
- Julli, M. (1999). "Ecotoxicity and chemistry of leachates from blast furnace and basic oxygen steel slags," *Aus. J. Ecotoxicol.* **5**, 123–132.
- Kelly, M. (2015). "Former Pasmenco worker reveals where tonnes of slag dumped around Cockle Bay and Speers Point park," *Newcastle Herald* 07 Jan 2015. Accessed 21 Mar 2017. <http://www.theherald.com.au/story/2803413/toxic-truth-slag-dumped-at-speers-point-park/>.
- Lottermoser, B. G. (2002). "Mobilization of heavy metals from historical smelting slag dumps, north Queensland, Australia," *Mineral. Mag.* **66**, 475–490.
- Mahieux, P.-Y., Aubert, J.-E., and Escadeillas, G. (2009). "Utilization of weathered basic oxygen furnace slag in the production of hydraulic road binders," *Constr. Build. Mater.* **23**, 742–747.
- Martínez-Sánchez, M. J., Navarro, M. C., Pérez-Sirvent, C., Marimón, J., Vidal, J., García-Lorenzo, M. L., and Bech, J. (2008). "Assessment of the mobility of metals in a mining-impacted coastal area (Spain, Western Mediterranean)," *J. Geochem. Explor.* **96**, 171–182.
- MINDAT (2017). Cordillera Mine, Kangaloolah, Tuena, Georgiana Co., New South Wales, Australia. <https://www.mindat.org/loc-77.html>.
- Morrison, A. L., and Gulson, B. L. (2007). "Preliminary findings of chemistry and bioaccessibility in base metal smelter slags," *Sci. Total Environ.* **382**, 30–42.
- Morrison, A. L., Swierczek, Z., and Gulson, B. L. (2016). "Visualisation and quantification of heavy metal accessibility in smelter slags: the influence of morphology on availability," *Environ. Pollut.* **210**, 271–281.
- Panayotova, M., Panayotov, V., and Sokolova, E. (2015). "Non-ferrous metals waste as metals' resource. Part 1 – availability, chemistry and mineralogy," *Sustain. Dev.* **3**, 85–93.
- Parbhakar-Fox, A., Lottermoser, B., and Bradshaw, D. (2013). "Evaluating waste rock mineralogy and microtexture during kinetic testing for improved acid rock drainage prediction," *Mineral. Eng.* **52**, 111–124.
- Piatak, N. M., Seal, R. R. II, Hammarstrom, J. M. (2004). "Mineralogical and geochemical controls on the release of trace elements from slag produced by base- and precious-metal smelting at abandoned mine sites," *Appl. Geochem.* **19**, 1039–1064.
- Piatak, N. M., Parsons, M. B., and Seal, R. R. II (2015). "Characteristics and environmental aspects of slag: a review," *Appl. Geochem.* **57**, 236–266.
- Romero, A., González, I., and Galán, E. (2006). "Estimation of potential pollution of waste mining dumps at Peña del Hierro (Pyrite Belt, SW,

- Spain) as a base for future mitigation actions,” *Appl. Geochem.* **21**, 1093–1108.
- Standards Australia. (1997). AS4439.3-1997. Wastes, sediments and contaminated soils – Part 3: Preparation of leachates – Bottle Leaching Procedure. <https://infostore.saiglobal.com/STORE/PreviewDoc.aspx?saleItemID=382308>.
- Ströbele, F., Wenzel, T., Kronz, A., Hildebrandt, L. H., and Markl, G. (2010). “Mineralogical and geochemical characterization of high-medieval lead-silver smelting slags from Wiesloch near Heidelberg (Germany) – an approach to process reconstruction,” *Archaeol. Anthropol. Sci.* **2**, 191–215.
- Strömberg, B., and Banwart, S. A. (1999). “Experimental study of acidity-consuming processes in mining waste rock: some influences of mineralogy and particle size,” *Appl. Geochem.* **14**, 1–16.
- Takeno, N. (2005). *Atlas of Eh-pH Diagrams. Intercomparison of Thermodynamic Databases*. (Geological Survey of Japan Open File Report No. 419). National Institute of Advanced Industrial Science and Technology. p 287.
- Xue, Y., Wu, S., Hou, H., and Zha, J. (2006). “Experimental investigation of basic oxygen furnace slag used as aggregate in asphalt mixture,” *J. Hazard. Mater.* **138**, 261–268.